Full length article

Regenerative effects of peptide nanofibers in an experimental model of Parkinson's disease

Melike Sever [a], Mesut Turkyilmaz [b], Cansu Sevinc [b], Aysen Cakir [c], Busra Ocalan [c], Mehmet Cansev [b,*], Mustafa O. Guler [a,*], Ayse B. Tekinay [a,*]

[a] Institute of Materials Science and Nanotechnology, National Nanotechnology Research Center (UNAM), Bilkent University, Ankara 06800, Turkey
[b] Department of Pharmacology, Uludag University School of Medicine, Bursa 16059, Turkey
[c] Department of Physiology, Uludag University School of Medicine, Bursa 16059, Turkey

ABSTRACT

Parkinson's disease (PD) is characterized by progressive degeneration of dopaminergic nigrostriatal neurons and reduction in striatal dopamine levels. Although there are few treatment options for PD such as Levodopa, they are used just to relieve and modify the symptoms. There are no therapies available for PD to slow down the degeneration process in the brain and recover the lost function. In this study, we used extracellular matrix (ECM) mimetic peptide amphiphile (PA) nanofibers as a potential therapeutic approach in a PD rat model. We demonstrated the effect of heparan sulfate mimetic and laminin mimetic PA nanofibers on reducing striatal injury and enhancing functional recovery after unilateral striatal injection of 6-hydroxydopamine (6-OHDA). The bioactive self-assembled PA nanofibers significantly reduced forelimb asymmetry, contralateral forelimb akinesia and d-amphetamine-induced rotational behavior in cylinder, stepping and rotation tests, respectively, in 6-OHDA-lesioned rats after 6 weeks. The behavioral improvement with PA nanofiber administration was associated with enhanced striatal dopamine and tyrosine hydroxylase content as well as reduced cleaved-Caspase-3 levels. Histological assessment also showed that PA nanofiber injection to the striatum resulted in better tissue integrity compared to control groups. In addition, PA nanofibers reduced the progressive cell loss in SH-SY5Y cells caused by 6-OHDA treatment. These data showed that the bioactive peptide nanofibers improve neurochemical and behavioral consequences of Parkinsonism in rats and provide a promising new strategy for treatment of PD.

Statement of Significance

Biomimetic nanomaterials bearing natural bioactive signals which are derived from extracellular matrix components like laminin and heparan sulfates provide promising therapeutic strategies for regeneration of the nervous system. However, no research has been reported exploring the use of biomimetic materials against degeneration in Parkinson's disease. In this work, we investigated potential therapeutic effects of heparan sulfate and laminin mimetic PA nanofibers on reduction of striatal injury in experimental Parkinson's disease model. PA nanofibers enhanced functional recovery associated with enhanced striatal dopamine and tyrosine hydroxylase content as well as reduced cleaved-Caspase-3 levels. Overall, this study shows the improvement in consequences of Parkinsonism in rats and provides a new platform for treatment of Parkinson's disease.

© 2016 Acta Materialia Inc. Published by Elsevier Ltd. All rights reserved.

1. Introduction

Neurodegenerative diseases caused by infection, stroke and acute trauma are the fourth cause of death in the world after cardiovascular diseases, cancer and stroke [1]. Among the neurodegenerative diseases, Parkinson's disease (PD) is the second most common neurodegenerative disease after Alzheimer's disease. PD is a severe, chronic and progressive disease associated with symptoms such as tremor, postural instability, rigidity and bradykinesia [2]. PD is char-

* Corresponding authors.
E-mail addresses: melikesever@gmail.com (M. Sever), turkyilmazmesut@gmail.com (M. Turkyilmaz), cnssvnc@gmail.com (C. Sevinc), aysencakir16@gmail.com (A. Cakir), busraocalan@gmail.com (B. Ocalan), mcansev@uludag.edu.tr (M. Cansev), moguler@unam.bilkent.edu.tr (M.O. Guler), atekinay@bilkent.edu.tr (A.B. Tekinay).

acterized by diminished levels of striatal dopamine as a consequence of dopaminergic neuron loss in the substantia nigra pars compacta. Beside the degeneration of dopaminergic neurons, Lewy body formation can be included into pathologic hallmarks of PD [3]. In addition, several studies have shown that activation of apoptosis is one of the mechanisms that underlie progressive striatal neurodegeneration [4–7]. Also, a recent study has provided strong evidence for this hypothesis by showing that *in vivo* suppression of Caspase-3, an apoptotic marker, by RNA interference in a rat model of PD reduced striatal dopaminergic cell loss and improved locomotor activity [8]. Millions of people in US and Europe suffer from PD, but the pharmaceutical agents used for PD treatment including levodopa, Monoamine oxidase-B inhibitors (selegiline and rasagiline), Catechol-O-methyl transferase inhibitors (tolcapone and entacapone) and dopamine agonists (pramipexole and ropinirole) just relieve and modify the symptoms. In addition, since they are administered orally, they can cause systemic toxicity with different adverse effects [9]. There are no therapies yet available for PD to slow down the degeneration process in the brain and recover the lost function. Besides these current strategies, there are various experimental approaches to improve the efficacy of currently available treatment strategies. Uses of adenosine A_{2A} receptor antagonists, glutamate receptor antagonists, monoamine oxidase inhibitors, anti-apoptotic agents, antioxidants and coenzyme Q10 are among the emerging pharmacotherapies at different stages of preclinical and clinical trials [10]. Also, there are several non-pharmacological approaches offering alternative strategies for the treatment of PD. Viral vectors were studied to silence the over-expressed defective genes considered as risk factors in PD or to transfer the genes such as glutamic acid decarboxylase gene [11]. Stem cell transplantation is another promising approach for the replacement of dopaminergic neurons progressively lost in PD. Induced pluripotent stem cells, neural stem cells and mesenchymal stem cells are the most commonly studied resources to generate dopaminergic neurons as a treatment strategy for PD [12]. However, there are some drawbacks for this technique such as selecting tumor-free cell type for transplantation, which limits the potential therapeutic benefits. Additionally, some surgical procedures are within the emerging techniques for PD treatment, including deep brain stimulation, pallidotomy and thalamotomy, especially for PD patients having severe disabling problems and not responding traditional treatment options. However, these procedures also have high risks and require close post-operative follow-up period [10].

Although repairing the damaged area in the brain is extremely challenging, recent advances in regenerative medicine and tissue engineering provide new therapeutic approaches for neurodegenerative disease treatment. Biomaterials, which are designed to interact with biological systems provide new platforms to replace the damaged neurons or slow down the progression of the diseases [13]. Biomaterial scaffolds can be modified with physical or/and chemical cues depending on aim of the study. Cell attachment, adhesion, migration and spreading as well as cell differentiation into specific lineages can be achieved through physical or chemical modification of the surface of the scaffold, including stiffness, topography, charge and interactions with extracellular-matrix (ECM) proteins or cells [14].

Laminins are heterotrimeric proteins and the major non-collagenous components of the basal lamina. They bind to cell membrane through interaction with integrin receptors on the cell surface, and by this way they can influence diverse biological activities including the adhesion, migration and differentiation [15]. Moreover, laminin has a fundamental role in axonal growth and myelination [16] and functions as a neurite-outgrowth promoting factor for peripheral and central neurons [17]. Laminin also interacts with other matrix elements such as heparan sulfate proteoglycans (HSPG) through noncovalent interactions, and laminin-HSPG complex was found to be involved in neurite outgrowth [18,19]. Heparan sulfates are highly sulfated glycosaminoglycans and function as cell–ECM interface to modify cell signaling. They also interact with various ECM molecules such as growth factors. They act as a reservoir of such growth factors and increase their local concentration [20–23].

The self-assembled peptide amphiphile (PA) nanofibers provide suitable platforms to mimic ECM. As a result of hydrophobic interaction of alkyl tails and β-sheet formation between PA molecules, they self-assemble into nanofibers in aqueous environment. Also, biochemical signals provided by a specific protein can be introduced into the nanofiber system through addition of bioactive epitopes into individual PA molecules instead of use of bulk protein [24]. The peptide sequences Ile-Lys-Val-Ala-Val (IKVAV) of cell-binding domain of laminin was discovered and found to facilitate neurite extension [25]. After the discovery of this small peptide sequence, IKVAV-carrying PAs were used in both *in vitro* and *in vivo* studies for neural differentiation [26] and spinal cord regeneration [27,28], respectively. We previously reported that combination of IKVAV-carrying PAs along with heparan-sulfate-mimicking PA nanofibers displayed dual bioactivity and promoted much longer neurite outgrowth compared to the scaffold with laminin-derived signals alone, even in the presence of inhibitory conditions provided by chondroitin sulfate proteoglycans [29]. Although bioactive PA nanofibers were shown to enhance *in vitro* neurite extension or peripheral nerve regeneration, there is no study on the therapeutic effects of bioactive PA nanofibers on Parkinson's disease.

Here we investigated whether these heparan sulfate and laminin mimetic PA nanofibers have potential therapeutic effect for both protection of SH-SY5Y cells against 6-hydroxydopamine (6-OHDA)-induced apoptosis in *in vitro* studies and for reducing striatal injury and enhancing dopaminergic nerve regeneration in experimental PD model. Six weeks following treatment with bioactive PA nanofibers, rats with 6-OHDA-induced Parkinsonism displayed improvements in behavioral functions, i.e., reductions in forelimb asymmetry, contralateral forelimb akinesia and d-amphetamine-induced rotational behavior in cylinder, stepping and rotation tests, respectively. Moreover, brain dopamine content and tyrosine hydroxylase (TH) levels increased, while cleaved-Caspase-3 levels decreased in rats treated with PA nanofibers compared to sucrose control. Histological assessment also showed that PA injection to the striatum provided better tissue integrity by reducing the progressive cell loss caused by 6-OHDA toxicity, which makes this bioactive nanofiber system a promising new platform for PD treatment.

2. Materials and methods

2.1. Materials

All protected amino acids, lauric acid, 4-[α-(2′,4′-dimethoxyphenyl) Fmoc-aminomethylphenoxyacetomidonorleucyl-MBHA resin (Rink amide MBHA resin), 2-(1*H*-benzotriazol-1-yl)-1,1,3,3-tetramethyluroniumhexafluorophosphate (HBTU) and diisopropylethylamine (DIEA) were purchased from Nova-Biochem, ABCR, or Sigma-Aldrich. 6-OHDA was purchased from Sigma Aldrich. Alamar Blue, viability assay reagents and other cell culture materials were purchased from Invitrogen. Apoptosis assay reagents were purchased from Biotium. All other chemicals and materials used in this study were purchased from Thermo Scientific or Sigma Aldrich.

2.2. Synthesis of PA molecules

PA molecules were synthesized on Rink Amide MBHA Resin or Fmoc-Glu(OtBu)-Wang Resin by using Fmoc-protected solid phase

peptide synthesis method. Amino acid couplings were performed with 2 equivalents of aminoacids activated with 1.95 equivalents of HBTU and 3 equivalents of DIEA for 2 h. Fmoc removal was performed with 20% piperidine–dimethylformamide (DMF) solution for 20 min. 10% acetic anhydride–DMF solution was used to permanently acetylate the unreacted amine groups after each coupling step. DMF and dichloromethane (DCM) were used as washing solvents after each step. *p*-Sulfobenzoic acid was coupled to the side chain of lysine to synthesize sulfonated PAs. A lysine residue with 4-methytrityl (Mtt) side chain protection was used for selective deprotection of amine groups. Mtt removal was performed by shaking resins for 5 min with TFA:TIS:H$_2$O:DCM in the ratio of 5:2.5:2.5:90. Cleavage of the PAs and protection groups from the resin was carried out with a mixture of TFA:TIS:H$_2$O in the ratio of 95:2.5:2.5 for 3 h. Excess TFA removal was carried out by rotary evaporation. PAs in the remaining solution were precipitated in ice-cold diethyl ether overnight. The precipitate was collected by centrifugation next day and dissolved in ultrapure water. This solution was frozen at -80 °C for 4 h and then lyophilized for 4–5 days. PAs were characterized by liquid chromatography–mass spectrometry (LC–MS). Mass spectrum was obtained with Agilent LC-MS equipped with Agilent 6530 Q-TOF with an ESI source and Zorbax Extend-C18 2.1 × 50 mm column for basic conditions and Zorbax SB-C8 4.6 × 100 mm column for acidic conditions. A gradient of (a) water (0.1% formic acid or 0.1% NH$_4$OH) and (b) acetonitrile (0.1% formic acid or 0.1% NH$_4$OH) was used. In order to remove residual TFA, positively-charged PAs were treated with 0.1 M HCl solution and lyophilized. To purify the peptides, Agilent preparative reverse-phase HPLC system equipped with Zorbax Extend-C18 21.2 × 150 mm column was used for basic conditions and Zorbax SB-C8 21.2 × 150 mm column was used for acidic conditions. A gradient of (a) water (0.1% TFA or 0.1% NH$_4$OH) and (b) acetonitrile (0.1% TFA or 0.1% NH$_4$OH) was used. All peptide batches were freeze-dried and reconstituted in ultrapure water at pH 7.4 before use.

2.3. Physical, mechanical and chemical characterization of self-assembled nanofiber network

2.3.1. Scanning electron microscopy (SEM)

PA nanofiber networks were observed by imaging with a scanning electron microscope (SEM). Oppositely charged PA solutions (1 wt%) were mixed in appropriate volume ratio (final volume being 30 µL) to produce gels with neutral charge. Gels were formed on silicon wafer and dehydrated by transferring to 20%, 40%, 60%, 80% and 100% v/v ethanol sequentially. They were critical point-dried afterwards by using Autosamdri 815B equipment from Tousimis. Dried PA gels were coated with 4 nm Au/Pd and SEM (FEI Quanta 200 FEG) images were taken by using an Everhart–Thornley Detector (ETD) at high vacuum mode at 5 keV beam energy

2.3.2. Scanning transmission electron microscope (STEM)

Samples for STEM imaging were prepared by mixing equal volumes of negatively and positively charged PA molecules with appropriate concentrations for charge neutralization and placing them on a 200-mesh carbon TEM grid for 10 min followed by 2 wt% uranyl acetate staining for 2 min and drying. STEM images at HAADF mode were acquired with FEI Tecnai G2 F30 TEM at 300 kV.

2.3.3. Circular dichroism (CD)

A JASCO J815 CD spectrometer was used at room temperature. Oppositely charged 2.5×10^{-4} M PA solutions were mixed in appropriate volume ratios (final volume being 500 µL) to produce nanofibers with net neutral charge. Measurements were carried out from 300 nm to 190 nm; data interval and data pitch being

0.1 nm, and scanning speed being 100 nm min^{-1}. All measurements were performed with three accumulations. Digital Integration Time (DIT) was selected as 1 s, band width as 1 nm, and the sensitivity was standard.

2.3.4. Oscillatory rheology

Oscillatory rheology measurements were performed with Anton Paar Physica RM301 Rheometer operating with a 25 mm parallel plate configuration at 25 °C. 250 µL total volume with 1 wt% of each PA component was carefully loaded onto the center of the lower plate and incubated for 10 min for gelation before measurement. After equilibration, the upper plate was lowered to a gap distance of 0.5 mm. Storage moduli (G′) and loss moduli (G″) values were scanned from 100 rad s^{-1} to 0.1 rad s^{-1} of angular frequency, with a 0.5% shear strain. Three samples were measured for each PA gel.

2.4. Cell culture and maintenance

SH-SY5Y cells (kindly provided by Prof. Dr. Fikrettin Sahin, Yeditepe University, Istanbul, Turkey) were used in cell culture experiments. They were cultured in 75 cm^2 flasks at 37 °C in a humidified incubator and supplied with 5% CO$_2$. Cells were maintained in 1:1 mixture of Eagle's minimum essential medium and F12 medium supplemented with 10% fetal bovine serum (FBS) and 1% penicillin/streptomycin. All cell experiments were carried out after reaching 90% confluency. The culture medium was changed every 3–4 days.

2.5. Drug treatment and viability assay

6-OHDA was dissolved in 0.3% ʟ-ascorbic acid/0.9% NaCl solution to create a stock concentration of 5 mM and was used at a final concentration of 25, 50, 100, 200 and 500 µM. SH-SY5Y cells were seeded at a density of 2×10^4 cells/well on 96-well plate and incubated for 24 h. Then, they were treated with 6-OHDA (25, 50, 100, 200 and 500 µM) for 24 h. Medium was discarded after 24 h of incubation and replaced with medium containing 10% Alamar blue. Blank group contained only Alamar blue medium without cells. After 3 h incubation at 37 °C, absorbance measurement was performed by using Spectramax M5 microplate reader at 570 and 600 nm as reference.

After determining the toxic dose, the viability test of SH-SY5Y cells was performed after 24 h of 6-OHDA treatment by using calcein-AM/ethidium homodimer 1 (EthD-1) staining. In brief, cells were incubated on PA-coated and uncoated 96 well-tissue culture plates at a density of 5×10^3 cells/well. After 24 h, the cells were exposed to 50 µM 6-OHDA dissolved in 0.3% ʟ-ascorbic acid/saline solution or vehicle (0.3% L-ascorbic acid/saline solution). After 24 h of incubation, cell medium was discarded; cells were washed with PBS and then incubated with 2 µM calcein-AM and 2 µM EthD-1 in PBS for 30 min at room temperature. Finally, five random images were taken at 100x magnification from each well for both qualitative and quantitative analysis by using Zeiss Axioscope fluorescence microscope. Cells were counted with Image J system for analyzing proliferation.

2.6. Flow cytometric analysis of apoptosis

Apoptosis in SH-SY5Y cells seeded on different PA combinations was measured using the Annexin V-FITC Apoptosis Detection kit. After 24 h incubation in 6-well plates at a density of 5×10^5 cells/well, the cells were exposed to 50 µM 6-OHDA dissolved in 0.3% ʟ-ascorbic acid/saline solution. After 24 h exposure to 6-OHDA, flow cytometry protocol for Annexin V and propidium iodide was performed. Medium was discarded; cells were washed

with cold PBS and resuspended in 1X annexin-binding buffer. 100 μL of 1X annexin-binding buffer per assay was added with 5 μL Alexa Fluor® 488 annexin V and 1 μL of 100 μg/mL propidium iodide. Cells were incubated at room temperature for 15 min. The stained cells were analyzed by flow cytometry, measuring the fluorescence emission at 530 nm (e.g., FL1) and >575 nm (e.g., FL3).

2.7. In vivo surgery

2.7.1. Animals

A total of 32 male Sprague Dawley rats (weighing 300–350 g) were housed individually in each cage with free access to food and water in a 12/12 h light/dark cycle. Experimental procedures conformed to the National Institute of Health Guide for the Care and Use of Laboratory Animals and were approved by the Local Ethics Committee on Experimental Animal Research of Uludag University, Bursa, Turkey (Approval ID: 2012-10/1).

2.7.2. Surgical procedures

Rats (n = 24) anesthetized with ketamine and xylazine (80 and 10 mg/kg, respectively) were placed into the stereotaxic apparatus (David Kopf Instruments, Tujunga, CA, USA). Their heads were shaved and a 2-cm incision was made on the skull under aseptic conditions ensured with 70% alcohol. After visualization of the bregma, two burr holes were drilled and hand-made guide cannulas (each 4 mm long) were placed (first one +0.48 mm anterior and second one -0.40 mm posterior to bregma). The cannulas were plugged and rats were returned to their cages after injection with a single dose of analgesic (buprenorphine; 0.05 mg/kg; s.c.). A group of rats (n = 8) underwent the same operation without placement of guide cannulas in order to serve as sham controls.

2.7.3. Intrastriatal lesioning with 6-OHDA and PA injection

24 h after the placement of guide cannulas, two injection apparatus were placed into the right striata of rats through the guide cannulas at the following coordinates: first at anteroposterior: +0.48 mm, mediolateral: −2.2 mm and vertical: −4.6 mm and second at anteroposterior: −0.40 mm, mediolateral: −4.0 mm and vertical: −6.0 mm according to the Rat Brain Atlas [30]. Freely-moving rats were injected intrastriatally through polyethylene tubing (PE 20; Becton Dickinson, Franklin Lakes, NJ, USA) attached to the apparatus at the given coordinates with either 8 μg of 6-OHDA (dissolved in saline containing 0.3% L-ascorbic acid, n = 16) or its solvent 0.3% L-ascorbic Acid (n = 8) at a volume of 2 μL using an injection pump with a flow rate of 1 μL/min. The cannulas were plugged and rats were followed up in individual cages with free access to food and water.

The dose and stereotaxic coordinates for 6-OHDA injections were selected from previous studies [31,32] which showed that this protocol is adequate for consistent depletion of approximately 70–80% of striatal dopamine and induce Parkinsonism in rats resembling the early phase of PD in clinical setting.

One week later, rats receiving intrastriatal 6-OHDA injections were tested for d-amphetamine-induced rotational behavior. Rats were injected intraperitoneally (i.p.) with d-amphetamine (5 mg/kg) and ipsilateral rotations between 15 and 45 min were recorded using an automated Rotameter system (TSE Systems, Germany). Initial behavioral task was performed in order to ensure that the unilateral striatal 6-OHDA lesion was established and the data were used to randomize the 6-OHDA-lesioned rats into two treatment groups (i.e., 6-OHDA + Sucrose [n = 8] and 6-OHDA + PA [n = 8] groups) with almost equal mean number of ipsilateral rotations (275 ± 11 and 275 ± 6, respectively) in this task. No rotational behavior was observed in rats in "Sham" and "L-Ascorbic Acid + PA" groups.

Rats were followed-up in their cages for three days after the initial rotational behavior task in order to allow for wash-out of d-amphetamine from the brain and then allocated into treatment groups as follows: (i) Sham group, (ii) L-Ascorbic Acid + PA group, (iii) 6-OHDA + Sucrose group and, (iv) 6-OHDA + PA group. Schematic representation of the experimental protocol has been presented in Fig. S2.

In rats receiving intrastriatal 6-OHDA or L-ascorbic acid injections, PA (1% aqueous solutions) or sucrose (0.25 M) injections were made using the same coordinates of the right striata through the existing guide cannulas. The 1% solutions dissolved in sucrose of both the heparan sulfate-mimicking (GAG) and laminin-derived (LN) PA nanofibers were injected consecutively by the help of the polyethylene tubing attached to the injection apparatus with a 5 min interval in between two injections. *In vivo* gel formation and further cell recruitment by LN-PA and GAG-PA were verified with preliminary studies (Fig. S3). After preliminary studies, same protocol was applied, and rats were then followed-up for a period of 6 weeks in individual cages with free access to food and water.

2.8. Behavioral analyses

2.8.1. Rotation test

On completion of 6 weeks, rats were subjected to rotational test as described above.

2.8.2. Cylinder test

Cylinder test was performed in order to evaluate the forelimb asymmetry in rats using a modified version [33] of the initially-described procedure [34]. Briefly, rats were put individually in a glass cylinder (21 cm diameter, 34 cm height) and video recorded for 5 min without prior habituation. To stimulate rats that showed little or no tendency to explore, the following methods were used in the given order: (i) turning the lights in the room on and off 2 ± 3 times; (ii) mildly shaking the cylinder for 2 ± 3 s; (iii) taking the rat out of the cylinder for approximately 30 s and then putting it back, as described previously [35]. Ipsilateral or contralateral forelimb touches to the cylinder wall were counted by a blinded observer from the video recordings.

2.8.3. Stepping test

Stepping test (Adjusting Steps Test) was performed in order to evaluate forelimb akinesia three times on the same day with 30 min intervals in between tests according to the procedure described previously [36]. Briefly, rats were held by the experimenter with one hand fixing the hindlimbs and slightly raising the hind part above the surface of a table with a width of 100 cm. The other hand fixed the forelimb not to be monitored. The rats were moved sideways with one paw touching the table at a speed of 100 cm/5 s first in the forehand and then in the backhand direction. The number of adjusting steps was counted for both paws in both directions by a blinded observer from the video recordings.

2.9. Animal perfusions and tissue acquisition

Three days after the behavioral tests to allow for the wash-out of d-amphetamine, rats in all groups were sacrificed either with or without transcardiac perfusion using 4% paraformaldehyde solution under ketamine and xylazine anesthesia. Brains were obtained and striata were excised in rats sacrificed without perfusion. Striata were homogenized using 0.4 N hydrochloric acid (HCl), and homogenates were kept for future analyses of dopamine, TH and cleaved-Caspase-3. Brains of rats obtained following paraformaldehyde perfusion were sectioned and processed for immunohistochemical analyses.

2.10. Histological analyses

Sections were deparaffinized in xylene and rehydrated in serial ethanol series for hematoxylin & eosin (H&E) staining according to the standard protocol. For immunohistochemistry experiments, sections were stained with anti-TH (1:250; Millipore AB152) and anti-Iba1 (1:2000 Sigma ab178846) antibodies. After primary antibody staining, horseradish peroxidase conjugated goat anti-rabbit secondary antibody (1:500; Millipore) was used followed by 3,3′-diaminobenzidine (DAB) staining. All samples were mounted onto glass slides using xylene based mounting medium. Digital images were acquired via Zeiss Axio Scope A1. Images were acquired by using 10x and 20x objectives.

2.11. Dopamine analyses

Dopamine contents of striata were analyzed using High Performance Liquid Chromatography (HPLC) coupled with an electrochemical detector and an analytical column as described previously [31]. The samples were run at a rate of 1 mL/min using a mobile phase containing 0.15 M Na_2HPO_4, 0.5 mM sodium octa-sulfate and 0.1 mM Na_2EDTA dissolved in 10% methanol solution.

2.12. Western blot analyses

Homogenates of striata were mixed with equal volumes of Laemmli loading buffer and boiled. Equal amounts of protein were loaded and separated using SDS-PAGE (4–20%; Bio-Rad, Hercules, CA, USA) and then transferred onto polyvinylidene fluoride (PVDF) membranes (Millipore, Billerica, MA, USA). The remaining binding sites were blocked with 4% non-fat dry milk (Carnation, Glendale, CA, USA) in Tris-buffered saline and Tween 20 (TBST). Membranes were then rinsed in TBST buffer and incubated overnight in TBST solution containing the primary antibody of interest (rabbit anti-TH [Millipore, Billerica, MA, USA] and rabbit anti-cleaved-Caspase-3 [Cell Signaling, Danvers, MA, USA]). Next day, blots were incubated with the appropriate peroxidase-linked secondary antibody followed by visualization of protein-antibody complexes using the enhanced chemiluminescence system (Millipore, Billerica, MA, USA) and digital images were developed using a Licor C-Digit blot scanner (LI-COR Biotechnology, Lincoln, NE, USA). Immunoreactive bands were compared densitometrically using the blot scanner's software. Membranes were stripped using a stripping buffer (Thermo Fisher Scientific, Rockford, IL, USA) and then incubated with mouse anti-βIII-tubulin (Sigma-Aldrich, St. Louis, MO, USA) antibody used as the loading control.

2.13. Statistical analyses

Statistical analyses were performed using Sigma Plot version 12.0 software. Data were expressed as mean ± standard error of mean. Comparisons between two groups were made using Student's t test and those between multiple groups were made by using one way ANOVA followed by post hoc Tukey test and one-
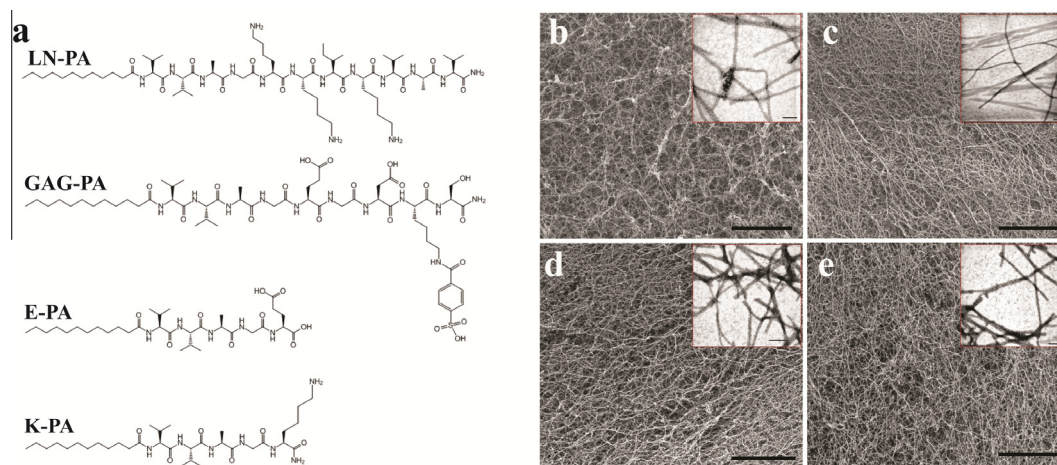
Fig. 1. Chemical structures of PA molecules (a). SEM images of LN-PA/GAG-PA (b), LN-PA/E-PA (c), K-PA/GAG-PA (d) and K-PA/E-PA (e) show nanofiber networks resembling the fibrous ECM structure. Scale bars are 3 μm in length. STEM images of all PA nanofibers formed at pH 7.4 are given in inner frames of panels b, c, d and e. Scale bars are 100 nm in length.
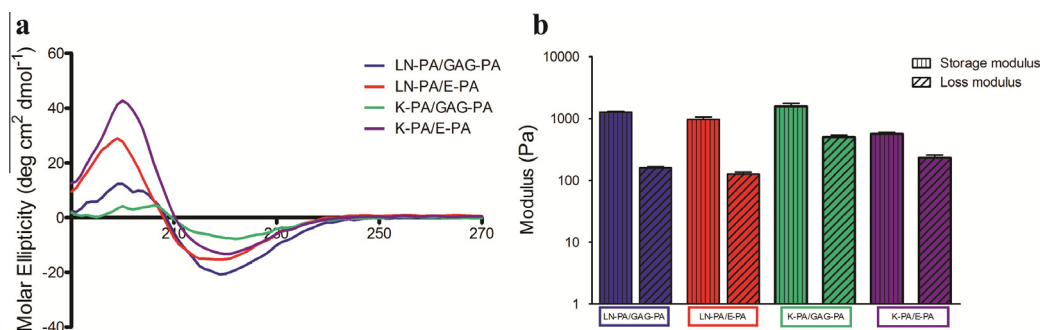
Fig. 2. Characterization of secondary structure of peptide nanostructures by circular dichroism (a). All PA combinations were found to have β-sheet secondary structure by circular dichroism analysis. Mechanical properties of PA gels measured by oscillatory rheology (b). Rheology results showed gelation as a result of nanofibrous network formation by all combinations at pH 7.4.

way ANOVA or two-way ANOVA with Bonferroni multiple comparison test. A p-value of less than 0.05 was considered significant ($^*p < 0.05$; $^{**}p < 0.01$; $^{***}p < 0.001$).

3. Results

3.1. Characterization of the peptide nanofibers

For both *in vitro* and *in vivo* studies, four different PA molecules were synthesized. All PA molecules had a hydrophobic alkyl tail composed of lauric acid and a β-sheet forming peptide sequence, VVAG. Lauryl-VVAGIKVAV-Am (LN-PA) was synthesized as laminin mimetic PA molecule and Lauryl-VVAGEGDK(pbs)S-Am (GAG-PA) was developed to mimic heparan sulfates with its sulfonate, hydroxyl and carboxylic acid groups incorporated as amino acid side chains. LN-PA/GAG-PA scaffolds bear two bioactive epitopes to mimic both laminin and heparan sulfates. The other two PA molecules used in this study were Lauryl-VVAGE (E-PA) and Lauryl-VVAGK-Am (K-PA) (Fig. 1a). These two PAs did not have any bioactive epitope sequences and they were used for gel formation with oppositely charged PAs to obtain K-PA/GAG-PA and LN-PA/E-PA nanofibers. K-PA/E-PA nanofibers were used as an epitope-free gel control. The PA molecules were synthesized by solid phase peptide synthesis, purified with preparative HPLC and characterized by LC-MS (Fig. S1). By SEM imaging, it was revealed that nanofiber networks in PA gels had morphological similarity to natural ECM that surrounds the cells in tissues (Fig. 1b, c, d and e). In addition, STEM imaging showed that all nanofibers were uniform in diameter (10–20 nm) and several micrometers in length (inner frames of Fig. 1b, c, d and e). We employed a circular dichroism spectrophotometer and observed predominant β-sheet structures with a chiral absorbance maximum at around 200 nm and minimum at around 220 nm

(Fig. 2a). To study the mechanical properties of PA gels, we used oscillatory rheology. Rheology results showed all PA combinations had higher storage modulus (G') than loss modulus (G''), verifying the gel formation at physiological pH (Fig. 2b).

3.2. In vitro studies

The dose response study was crucial to determine the IC_{50} value of the 6-OHDA concentration. Different concentrations of 6-OHDA (0–750 μM) were applied to SH-SY5Y cells and 6-OHDA-induced cytotoxicity was evaluated using Alamar blue assay. Viability of SH-SY5Y cells markedly decreased following 24 h incubation with an increasing concentration of 6-OHDA (Fig. 3a). A concentration of 50 μM for 6-OHDA was chosen for subsequent experiments since this concentration adequately decreased cell viability to about 50% (p < 0.001). Cellular viability of SH-SY5Y cells treated with either 6-OHDA or vehicle was assessed by calcein-AM/ethidium homodimer 1 staining, by comparison to cells that were cultured on different PA nanofibers. Results demonstrated that the cell viability on LN-PA/GAG-PA nanofibers was the highest and significantly greater than other PA combinations (Fig. 3b). Using Annexin V and the propidium iodide double-staining system, the Annexin V⁻/propidium iodide⁻ population was considered as normal healthy cells, while Annexin V⁺/propidium iodide⁻ cells were taken as a measurement of early apoptosis and Annexin V⁺/propidium iodide⁺ as late apoptosis. After 24 h of incubation of cells seeded on different PA combinations and tissue culture plate (TCP) with 6-OHDA, results showed that the percentage of live cells in LN-PA/GAG-PA group was significantly higher than other groups (p < 0.001) (Fig. 3c). Also, percentage of late apoptotic cells was lowest in LN-PA/GAG-PA group compared to other groups (p < 0.001), which showed that LN-PA/GAG-PA combination indicates a potentially favorable outcome for *in vivo* studies.
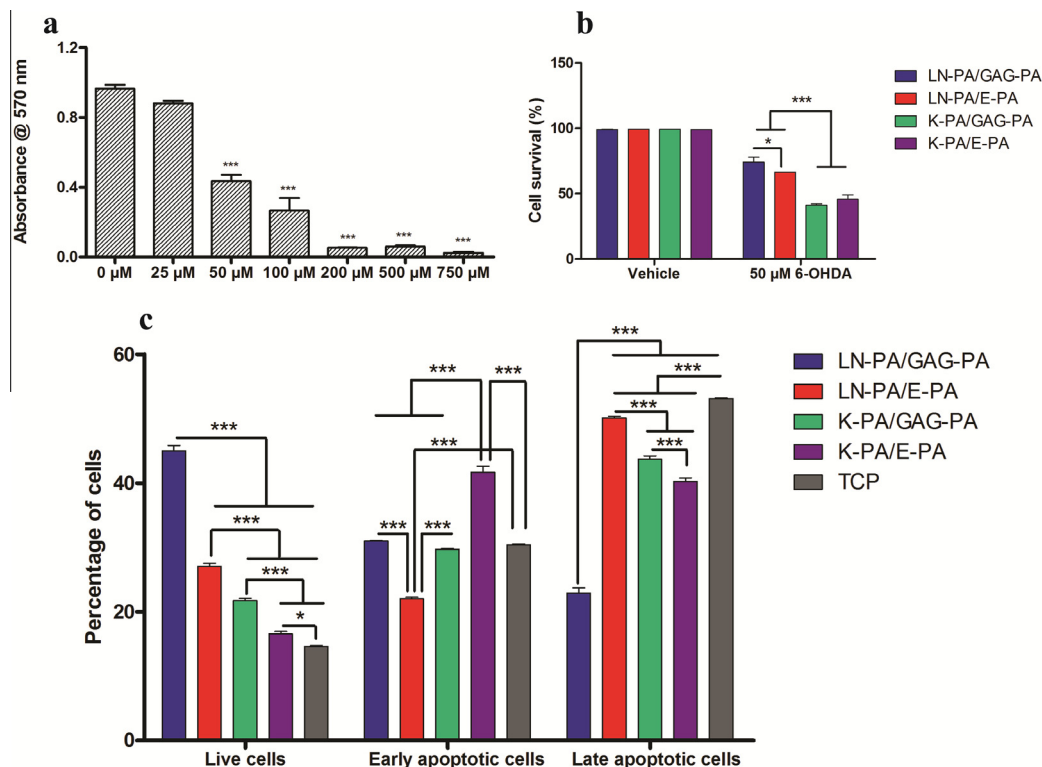
Fig. 3. Effects of PA nanofibers on SH-SY5Y cell viability after 6-OHDA treatment. Concentration-dependent toxicity of 6-OHDA in SH-SY5Y cells determined by Alamar blue assay (a). Viability of SH-SY5Y cells when cultured on peptide nanofibers in the presence or absence of 50 μM 6-OHDA for 24 h analyzed by calcein/ethidium homodimer live−dead assay (b). Cell apoptosis on different PA combinations and TCP after 24 h of culture was tested by flow cytometry analysis (c). Values represent mean ± SEM (*p < 0.05, ***p < 0.001). (For interpretation of the references to colour in this figure legend, the reader is referred to the web version of this article.)

3.3. PA nanofibers provide significant improvements in behavioral functions

In cylinder test, rats in Sham, L-Ascorbic Acid + PA, 6-OHDA + Sucrose and 6-OHDA + PA groups made 8.5 ± 2, 8.3 ± 1, 7.8 ± 1 and 7.8 ± 1 touches with only the ipsilateral forelimb, respectively (Fig. 4a), and 45.5 ± 8, 45.3 ± 10, 30.8 ± 6 and 36.5 ± 6 touches with both forelimbs at the same time, respectively (Fig. 4c). The number of touches with only the ipsilateral forelimb and both forelimbs did
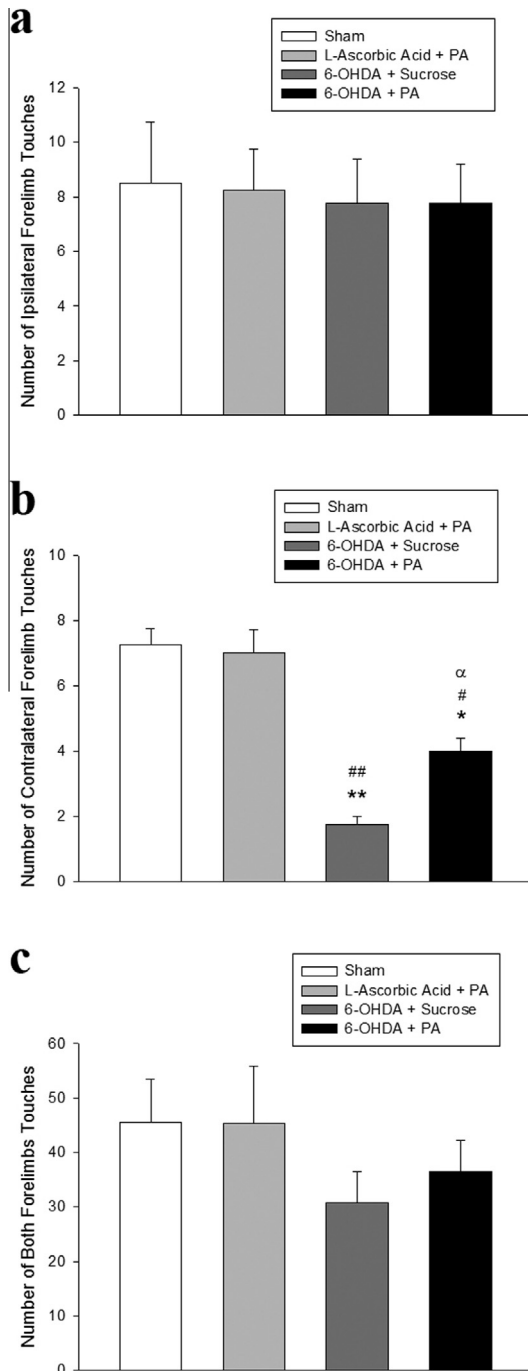
Fig. 4. Changes in forelimb asymmetry evaluated by cylinder test. Number of forelimb touches to the surface of a cylinder with the rats' ipsilateral (a), contralateral (b) and both forelimbs (c) was counted. Data are expressed as mean ± standard error of means (SEM). Statistical analyses were performed by one way ANOVA followed by post hoc Tukey test. $^{*}p < 0.05$ and $^{**}p < 0.001$ vs. sham group; $^{#}p < 0.05$ and $^{##}p < 0.001$ vs. L-ascorbic acid + PA group; and $^{\alpha}p < 0.05$ vs. 6-OHDA + sucrose group.

not differ significantly among groups. On the other hand, compared to sham group (7.36 ± 0.5), number of contralateral touches was reduced significantly in 6-OHDA + Sucrose (1.8 ± 0.3; $p < 0.001$) group while it was increased significantly in 6-OHDA + PA group to 4 ± 0.8 (Fig. 4b).

Number of adjusting steps that the rats made did not differ significantly among groups when rats were moved sideways on their ipsilateral forelimb both in the ipsilateral and contralateral directions (Fig. 5a, b). On the contrary, number of adjusting steps was reduced significantly in rats in the 6-OHDA + Sucrose group when rats were moved sideways on their contralateral forelimb in the ipsilateral (9.7 ± 1; $p < 0.05$) (Fig. 5c) and contralateral (3.5 ± 0.2; $p < 0.001$) (Fig. 5d) directions compared with those in Sham group (14.4 ± 0.4 in the ipsilateral and 10.4 ± 0.5 in the contralateral direction). Compared with the 6-OHDA + Sucrose group, number of contralateral touches tended to increase (11.2 ± 1) and did significantly increase (6.2 ± 0.1; $p < 0.05$) in rats in the 6-OHDA + PA group when rats in this group were moved sideways on their contralateral forelimb in the ipsilateral (Fig. 5c) and contralateral (Fig. 5d) direction, respectively.

Rotational behavior was tested initially in 6-OHDA-lesioned rats in order to randomize rats to 6-OHDA + Sucrose and 6-OHDA + PA groups by ensuring similar number of ipsilateral rotations (275 ± 11 and 275 ± 6, respectively) (Fig. 6a). Six weeks after treatment, rats in 6-OHDA + Sucrose group displayed almost identical number of ipsilateral rotations (273 ± 7) to that observed before treatment onset while, on the contrary, number of ipsilateral rotations were reduced significantly to 226 ± 2 ($p < 0.001$) in rats in the 6-OHDA + PA group after 6 weeks of treatment (Fig. 6b).

3.4. PA nanofibers support tissue integrity and enhance cell migration towards striatum

In order to monitor morphology of striatum, H&E staining was carried out on brain sections taken from the rat brains at the end of 6 weeks. H&E staining revealed that there was tissue loss due to injection of 6-OHDA in 6-OHDA + Sucrose sections. Entry of the cannula can be observed clearly and there was almost no cell accumulation towards the damaged area. In contrast, PA injection to the striatum provided better tissue integrity compared to sucrose control. The gel was degraded at the end of 6 weeks, and cells accumulated towards the injury site and covered this region (Fig. 7). This result shows that the PA gel helps to maintain tissue integrity in 6-OHDA injected striata. For characterization of cells within the injury site, immunohistochemistry against Iba-1 was performed, and cells that accumulated towards the injection site in gel in 6-OHDA + PA groups were characterized as microglia when staining positively for Iba-1 (Fig. 8).

3.5. PA nanofibers enhance striatal dopamine content

Intrastriatal 6-OHDA lesioning reduced the dopamine content in the ipsilateral striatum from 0.94 ± 0.05 pmol/µg protein in Sham group to 0.44 ± 0.02 pmol/µg protein ($p < 0.001$) in 6-OHDA + Sucrose group (Fig. 9). PA treatment enhanced this reduced dopamine content significantly to 0.75 ± 0.01 pmol/µg protein ($p < 0.05$) (Fig. 9). Dopamine content of ipsilateral striatum did not differ in L-Ascorbic Acid + PA group (0.92 ± 0.05 pmol/µg protein) compared with that in Sham group.

### 3.6. PA nanofibers enhance TH levels and TH immunoreactivity

Similarly to dopamine levels, TH levels were reduced significantly in rats in 6-OHDA + Sucrose group by 79% ($p < 0.001$) compared with the Sham group (Fig. 10A). The fall in striatal

TH was less pronounced, although significant, in 6-OHDA + PA group (by 49%; $p < 0.001$) compared with Sham. On the other hand, TH levels were significantly greater in 6-OHDA-lesioned rats treated with PA compared with those receiving Sucrose ($p < 0.05$) (Fig. 10A).

Immunohistochemistry against TH also showed that TH-immunoreactivity almost disappeared in striatal sections, and 6-OHDA injection caused progressive dopaminergic cell loss in 6-OHDA + Sucrose group both in injury site and around this region. However, this progressive cell loss was inhibited by PA gel in 6-OHDA + PA group. (Fig. 10B).

3.7. PA nanofibers reduce apoptosis

We investigated the extent of apoptosis by analyzing cleaved-Caspase-3 levels in the lesioned striatum. Compared with sham group, levels of cleaved-Caspase-3 almost doubled in rats with 6-OHDA lesion which received Sucrose intrastriatally ($196 \pm 9\%$; $p < 0.001$) while the increase in cleaved-Caspase-3 was less pronounced in parkinsonian rats which received PA ($156 \pm 8\%$; $p < 0.001$) (Fig. 11). Strikingly, the reduction of cleaved-Caspase-3 levels in PA group was significant compared to Sucrose group ($p < 0.001$).
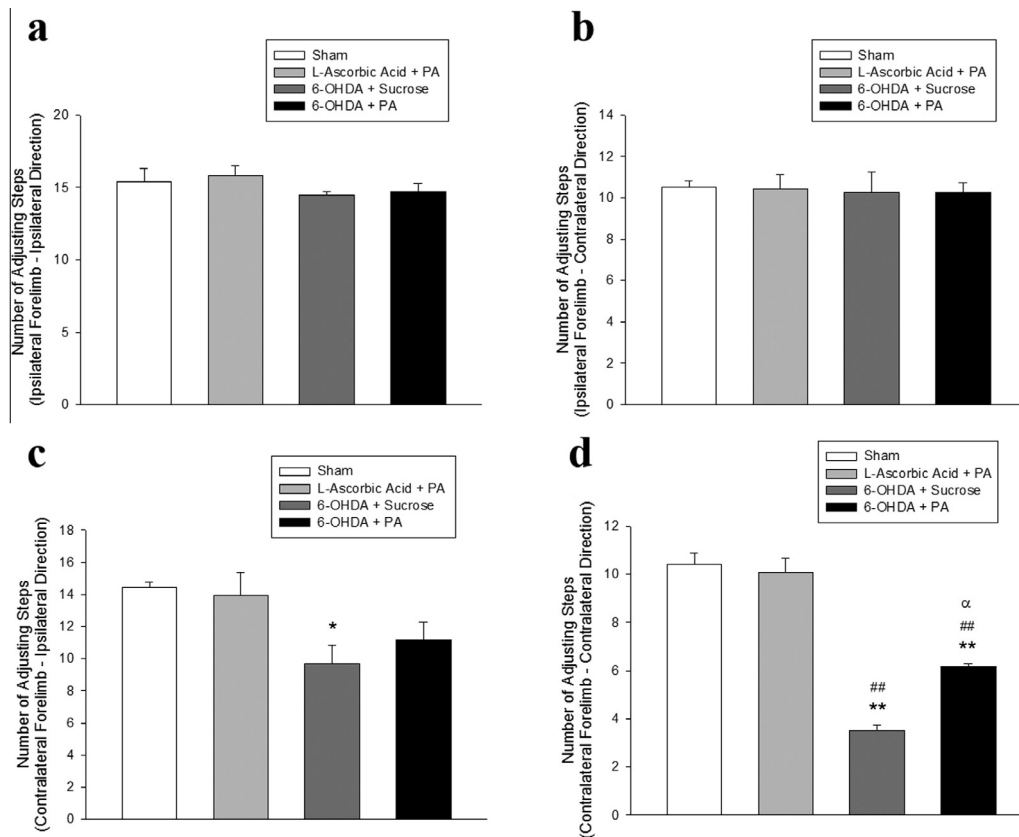
Fig. 5. Changes in forelimb akinesia evaluated by stepping test. Number of adjusting steps that the rats made were counted when rats were moved sideways with one paw touching the table at a speed of 100 cm/5 s first in the forehand and then in the backhand direction. Figure shows mean number of adjusting steps made by the rat on its ipsilateral forelimb towards ipsilateral direction (a), ipsilateral forelimb towards contralateral direction (b), contralateral forelimb towards ipsilateral direction (c) and contralateral forelimb towards contralateral direction (d). Data were expressed as mean ± SEM of three tests performed with 30 min intervals on the same day. Statistical analyses were performed by one way ANOVA followed by post hoc Tukey test. **$p < 0.001$ vs. Sham group; ##$p < 0.001$ vs. ʟ-Ascorbic Acid + PA group; and ᵅ$p < 0.05$ vs. 6-OHDA + Sucrose group.
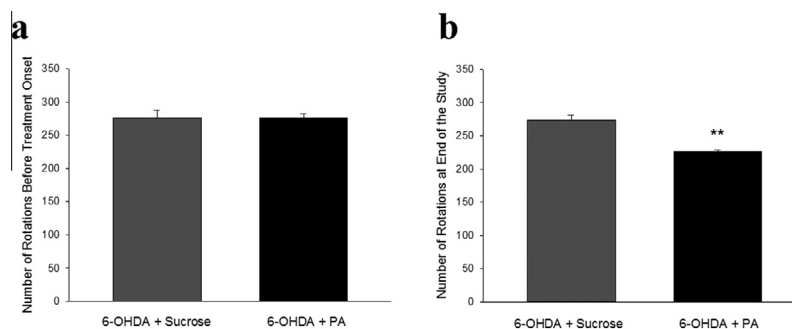
Fig. 6. Changes in rotational behavior evaluated by rotameter. Rats were injected intraperitoneally (i.p.) with d-amphetamine (5 mg/kg), and ipsilateral rotations between 15 and 45 min were recorded using an automated Rotameter system. Initial behavioral task (a) was performed in order to ensure that the unilateral striatal 6-OHDA lesion was established and the data were used to randomize the 6-OHDA-lesioned rats into two treatment groups while the test was repeated 6 weeks after administration of PA nanofibers (b). Data are expressed as mean ± SEM. Statistical analyses were performed by Student's *t* test. **$p < 0.05$ vs. 6-OHDA + Sucrose group.
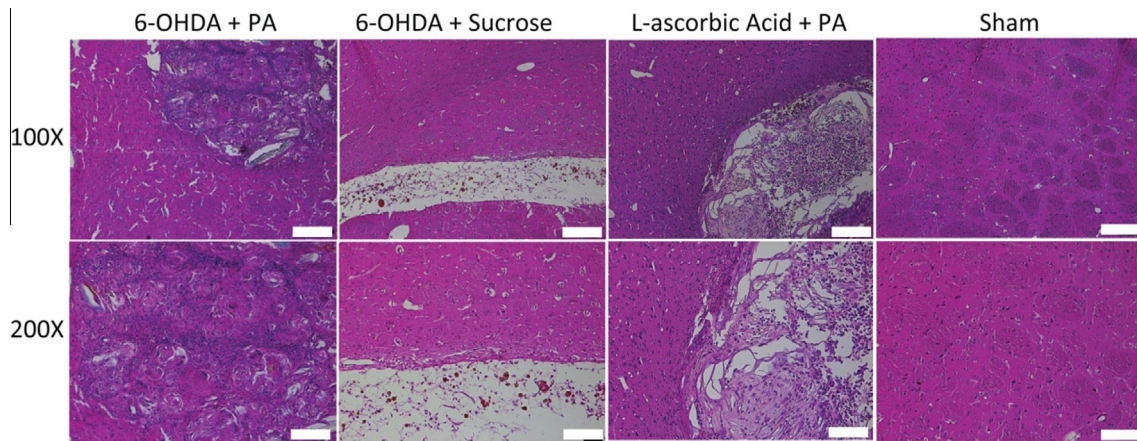
Fig. 7. H&E staining of striata of rat brain sections at postoperative week 6. The sections of 6-OHDA + PA group were compared with that of sham, L-Ascorbic Acid + PA and 6-OHDA + Sucrose groups. Images were taken with 100X (Scale bars 200 μm in length) and 200X magnifications (Scale bars 100 μm in length).
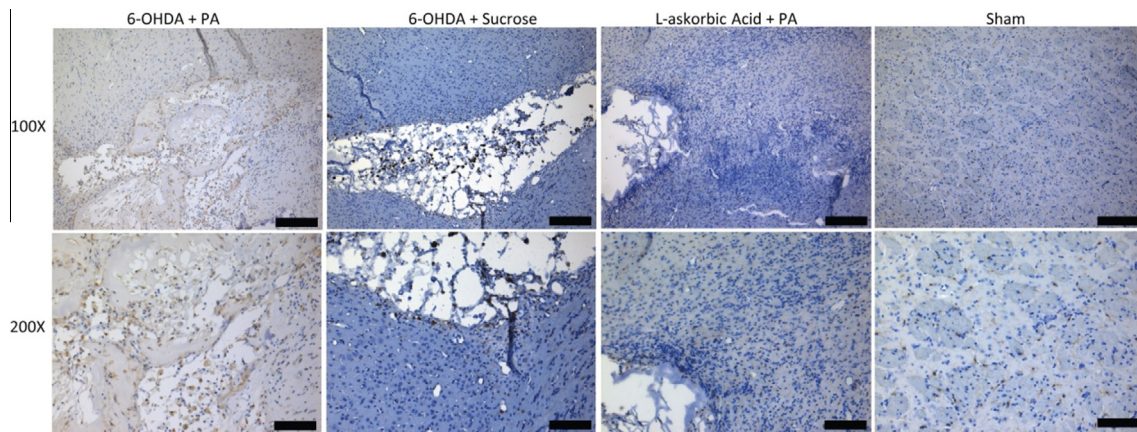
Fig. 8. Immunohistochemistry against Iba-1 protein for rat brain sections at postoperative week 6. The sections of 6-OHDA + PA group were compared with that of Sham, L-Ascorbic acid + PA and 6-OHDA + Sucrose groups. Images were taken with 100X (Scale bars 200 μm in length) and 200X magnifications (Scale bars 100 μm in length).
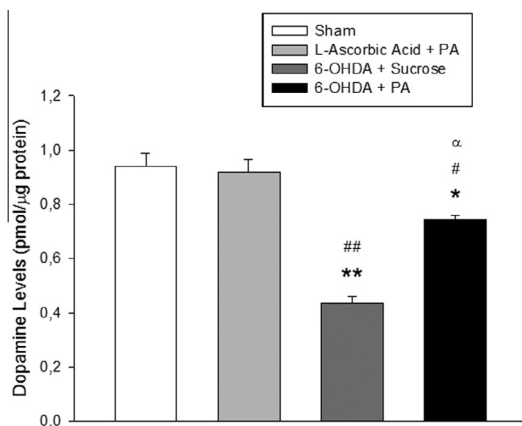
Fig. 9. Levels of dopamine in lesioned striatum. Data are expressed as mean ± SEM. Statistical analyses were performed by one way ANOVA followed by post hoc Tukey test. $^*p < 0.05$ and $^{**}p < 0.001$ vs. Sham group; $^{\#}p < 0.05$ and $^{\#\#}p < 0.001$ vs. L-Ascorbic Acid + PA group; and $^{\alpha}p < 0.05$ vs. 6-OHDA + Sucrose group.

4. Discussion

PD is a chronic and progressive disorder affecting millions of people worldwide, and is manifested by motor symptoms such as tremor, bradykinesia, rigidity and postural instability. Symptoms arise initially as a consequence of degeneration of dopaminergic nigrostriatal neurons and reduction in striatal dopamine levels. Etiopathogenesis of PD includes various factors such as alpha-synuclein dysfunction, ubiquitin-proteasome system, lysosomal autophagy, endoplasmic reticulum stress, mitochondrial dysfunction, oxidative stress and calcium dysregulation [37]. Several alternative treatments are being tested both experimentally and clinically which target one or more of these ethiopathogenetic factors. Recently, enhanced apoptotic cell death has been suggested as an underlying mechanism for progressive striatal neurodegeneration [4–7].

Although current treatment approaches, including the gold standard L-Dopa, provide benefit in particularly early stages of the disease, these approaches have been used just to relieve the symptoms and they become inadequate in the late stages. There are no therapies for PD to slow down the degeneration process in the brain and recover the lost function yet. Therefore, recent advances in regenerative medicine and tissue engineering would be a good therapeutic approach for neurodegenerative diseases like PD. In this study, we utilized a bioactive peptide nanofiber system for enhancing neuroprotection against 6-OHDA-induced cytotoxicity both *in vitro* and *in vivo*. These nanofibers are formed through the self-assembly of short bioactive PA molecules (LN-PA and GAG-PA) that were designed to mimic both laminin and heparan sulfate, since they can induce neurite outgrowth [29]. Heparin was also shown to stabilize laminin networks which lead to better neuritogenesis through heparin–laminin complexes [38].

Besides biological cues, physical properties are also important to enhance the efficacy of the PA nanofibers used in this study. PA scaffolds used in this study are similar to ECM of neural tissues in terms of physical appearance of fibrous networks. When designing a scaffold for nervous tissue, the mechanical characteristics of the scaffold should be similar to that of brain tissue, which is about 1 kPa [39]. Rheological measurements confirmed that all PA combinations formed gels and displayed similar properties to nervous tissue.

We observed that viability of the cells on all surfaces was comparable at the end of 24 h, which emphasizes the biocompatibility of all PA nanofiber combinations for SH-SY5Y cells, which are used as *in vitro* cell model of dopaminergic neurons in PD. When we treated the cells with 6-OHDA for 24 h, the highest viability was observed in SH-SY5Y cells seeded on LN-PA/GAG-PA combination, which was significantly different from other surfaces. For detailed analysis of neuroprotection of LN-PA/GAG-PA combination, we checked apoptosis using Annexin V FITC and propidium iodide assay, which indicates specific morphologic features of apoptosis

to categorize type of cell death. Flow cytometry analyses showed that live cells were significantly highest in LN-PA/GAG-PA combination, which is compatible with calcein/ethidium homodimer live-dead assay results. In contrast, late apoptotic cells were lowest in this group, which was significantly different from other PA combinations and TCP. These results make LN-PA/GAG-PA combination the best option for further *in vivo* studies.

The 6-OHDA model of nigral injury has been utilized for decades as a clinical experimental model of PD [40]. Intrastriatal injection of 6-OHDA leads to retrograde and progressive degeneration, thus providing a useful approach to study neuroprotective and neuroregenerative effects of experimental studies. We used this model for *in vivo* studies and injury was verified with amphetamine-induced rotational test. After injury, we injected bioactive gel as a therapeutic agent to prevent toxic effect of 6-OHDA. It was observed that the peptide gel disintegrated and provided cell accumulation towards the injury site, which was apparent 21 days after the PA gel injections (Fig. S3). These cells were characterized as microglia through immunohistochemical analysis
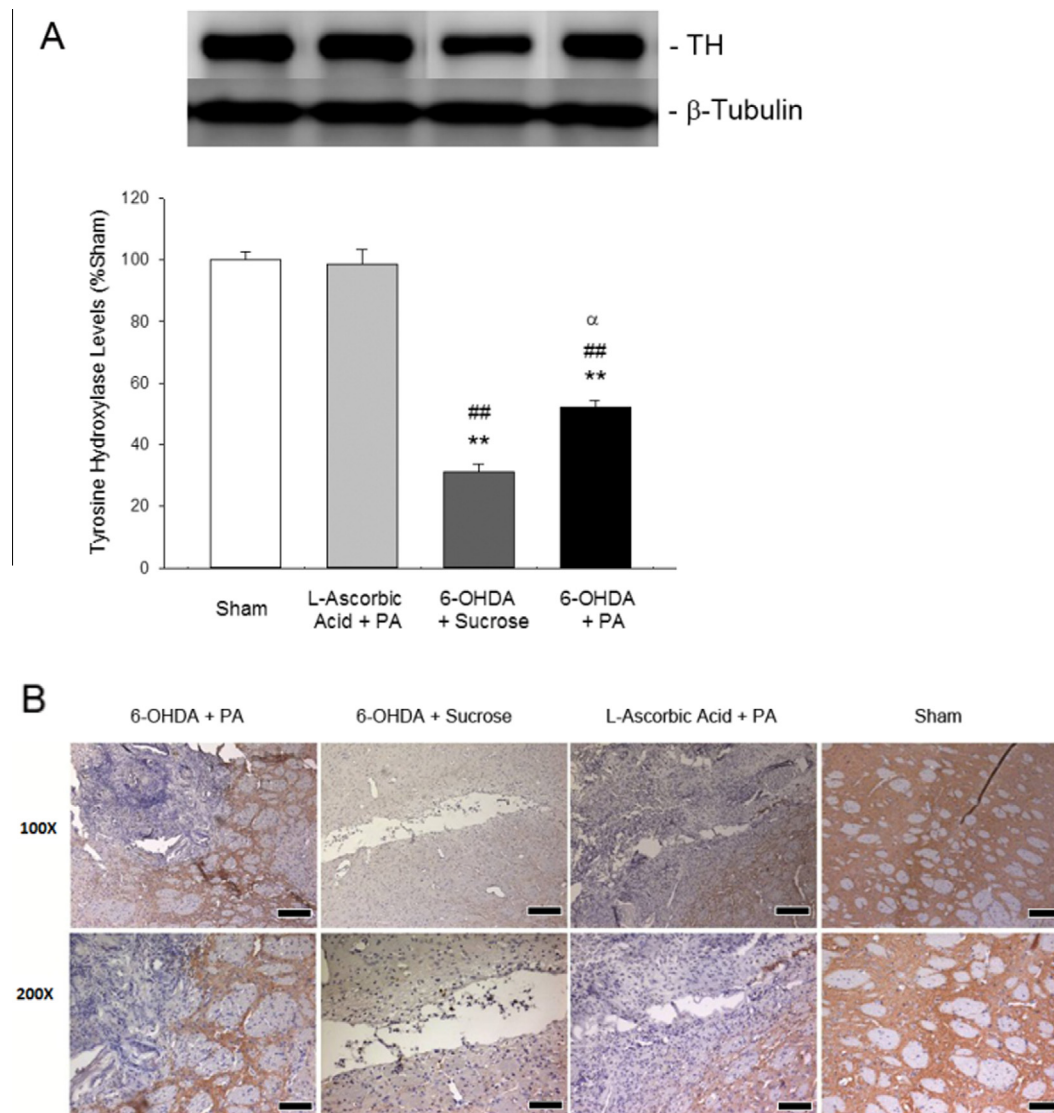
Fig. 10. Levels of Tyrosine Hydroxylase (TH) analyzed by Western blot (A) and immunohistochemistry (B) in lesioned striatum. Data obtained in Western blot analyses (A) are expressed as mean ± SEM. Statistical analyses were performed by one way ANOVA followed by post hoc Tukey test. $^{**}p < 0.001$ vs. Sham group; $^{##}p < 0.001$ vs. L-Ascorbic Acid + PA group; and $^{\alpha}p < 0.05$ vs. 6-OHDA + Sucrose group. In immunohistochemical analyses, no staining against TH was observed in 6-OHDA + Sucrose group, while TH protein immunostaining was detected in the lesion area in 6-OHDA + PA group at an extent similar with that observed in L-Ascorbic Acid + PA group (B). Images were taken with 100X (Scale bars 200 μm in length) and 200X magnifications (Scale bars 100 μm in length).
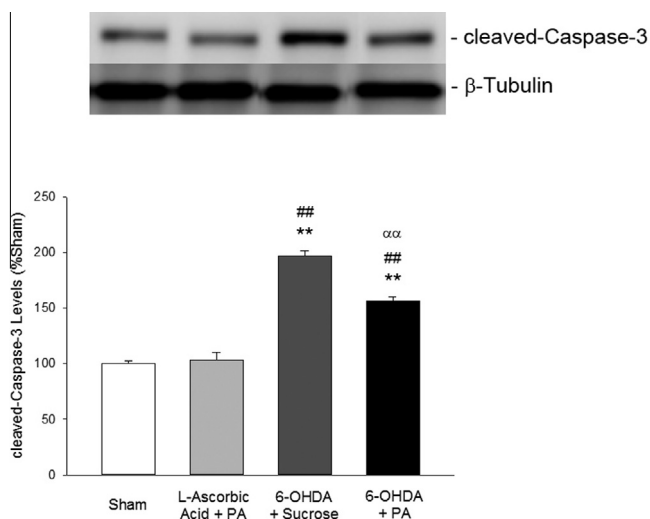
Fig. 11. Levels of cleaved-Caspase-3 analyzed by Western blot. Data were expressed as mean ± SEM. Statistical analyses were performed by one way ANOVA followed by post hoc Tukey test. $^{**}p < 0.001$ vs. Sham group; $^{##}p < 0.001$ vs. L-Ascorbic Acid + PA group; and $^{\alpha\alpha}p < 0.001$ vs. 6-OHDA + Sucrose group.

against Iba-1, which is a calcium-binding protein and plays a role in regulation of microglial function. Microglial activation occurs in central nervous system as a result of several pathological situations including inflammation and degeneration [41,42]. Microglia can serve for removal of deleterious debris by phagocytic activity after brain injury or neurodegeneration and contribute to neuroprotection by releasing neurotrophic factors [43,44]. In addition, properly-activated microglia have been shown to restrict the lesion area and provide protection in an experimental model of PD [45]. Therefore, we suggest that PA nanofibers behaved as a scaffold mimicking the ECM which enabled cell accumulation to alleviate the extent of the injury created by 6-OHDA injection.

Besides recruiting microglia, another mechanism by which PA nanofibers provide protection in the 6-OHDA rat model of PD might be represented by their anti-apoptotic activity, as shown in our study by reduction of the enhanced cleaved-Caspase-3 levels in vehicle (Sucrose) group. In good accord, a recent study showed that silencing of Caspase-3 by RNA interference reduced striatal dopaminergic cell loss and increased locomotor activity in a rat model of PD [8], suggesting a role for apoptosis in the pathogenesis of PD. The reduction in cleaved-Caspase-3 levels observed in our study therefore contributes to our understanding of how PA nanofibers provide protection in a rat model of PD, as has been shown previously for IKVAV-carrying epitopes in spinal cord injury [28].

The beneficial effect of PAs in the current model was represented biochemically by increased dopamine and TH content of the 6-OHDA-lesioned striatum. In addition, PA treatment also improved behavioral consequences of the experimental parkinsonian lesion by reducing forelimb asymmetry and akinesia as well as decreasing the number of ipsilateral rotations induced by systemic d-amphetamine administration. The ameliorations in biochemical and behavioral parameters observed in the present study are probably associated with anti-apoptotic and microglia-recruiting activities of PA nanofibers which resulted in restriction of the 6-OHDA lesion and enabled survival of a greater number of dopaminergic neurons, as has been shown in in vitro experiments.

Overall, striatal microinjection of heparan sulfate and laminin mimetic PA nanofibers reduced striatal pathology and improved behavioral consequences in a rat model of PD by providing cell recruitment, preventing progressive cell loss and reducing apopto-

sis. This is the first study that reports beneficial effects of bioactive PA nanofibers in the treatment of neurodegenerative disorders and these PA nanofibers may be used as a promising new strategy for the treatment of PD.

5. Conclusion

Herein we utilized a bioactive PA nanofiber gel system for therapeutic effect in both for SH-SY5Y cell culture and experimental PD model. In vitro results revealed that laminin-derived peptide signals along with heparan-sulfate-mimicking epitope were found to provide better viability through decreasing the apoptosis after 6-OHDA treatment. Furthermore, in vivo results showed that this scaffold is effective on reducing striatal injury and enhancing functional recovery after unilateral striatal injection of 6-OHDA. Also, histological analyses demonstrated that PA gel helped to maintain tissue integrity in 6-OHDA injected striata and prevented progressive dopaminergic cell loss around the damaged area. Overall, incorporation of heparan sulfate and laminin mimetic epitopes into PA nanofiber system decreased the toxic effect of 6-OHDA and provided better functional outcomes. This is the first study that reports the protective effects of PA nanofibers in a neurodegenerative disease model, which makes this system a promising therapeutic approach against degeneration in PD, but there still is a need for further studies to see the effects of these PA nanofibers on genetic model before the clinical trials since genetic models may better simulate the mechanisms underlying the genetic forms of PD. In addition, further studies on reducing the invasiveness of this technique would be beneficial prior to testing it in clinical settings.

Appendix A. Supplementary data

Supplementary data associated with this article can be found, in the online version, at http://dx.doi.org/10.1016/j.actbio.2016.09.011.

References

[1] O. Union, Health at a Glance, OECD Publishing, Europe, 2010.
[2] L.M.L. de Lau, M.M.B. Breteler, Epidemiology of Parkinson's disease, Lancet Neurol. 5 (6) (2006) 525–535.
[3] T.M. Dawson, V.L. Dawson, Molecular pathways of neurodegeneration in Parkinson's disease, Science 302 (5646) (2003) 819–822.
[4] N. Lev, E. Melamed, D. Offen, Apoptosis and Parkinson's disease, Prog. Neuropsychopharmacol. Biol. Psychiatry 27 (2) (2003) 245–250.
[5] N.A. Tatton, Increased caspase 3 and Bax immunoreactivity accompany nuclear GAPDH translocation and neuronal apoptosis in Parkinson's disease, Exp. Neurol. 166 (1) (2000) 29–43.
[6] W.G. Tatton, R. Chalmers-Redman, D. Brown, N. Tatton, Apoptosis in Parkinson's disease: signals for neuronal degradation, Ann. Neurol. 53 (Suppl. 3) (2003) S61–S70. discussion S70–S72.
[7] K. Venderova, D.S. Park, Programmed cell death in Parkinson's disease, Cold Spring Harb. Perspect. Med. 2 (8) (2012).
[8] Y. Liu, Y.B. Guo, S. An, Y.Y. Kuang, X. He, H.J. Ma, J.F. Li, J. Lv, N. Zhang, C. Jiang, Targeting Caspase-3 as dual therapeutic benefits by RNAi facilitating brain-targeted nanoparticles in a rat model of Parkinson's disease, PLoS One 8 (5) (2013).
[9] C. Ossig, H. Reichmann, Treatment strategies in early and advanced Parkinson disease, Neurol. Clin. 33 (1) (2015) 19–37.
[10] F.I. Tarazi, Z.T. Sahli, M. Wolny, S.A. Mousa, Emerging therapies for Parkinson's disease: from bench to bedside, Pharmacol. Ther. 144 (2) (2014) 123–133.

[11] M.G. Kaplitt, A. Feigin, C. Tang, H.L. Fitzsimons, P. Mattis, P.A. Lawlor, R.J. Bland, D. Young, K. Strybing, D. Eidelberg, M.J. During, Safety and tolerability of gene therapy with an adeno-associated virus (AAV) borne GAD gene for Parkinson's disease: an open label, phase I trial, Lancet 369 (9579) (2007) 2097–2105.

[12] M.H. Fu, C.L. Li, H.L. Lin, P.C. Chen, M.J. Calkins, Y.F. Chang, P.H. Cheng, S.H. Yang, Stem cell transplantation therapy in Parkinson's disease, Springerplus 4 (2015).

[13] Y. Zhong, R.V. Bellamkonda, Biomaterials for the central nervous system, J. R. Soc. Interface 5 (26) (2008) 957–975.

[14] B. Mammadov, M. Sever, M.O. Guler, A.B. Tekinay, Neural differentiation on synthetic scaffold materials, Biomater. Sci. UK 1 (11) (2013) 1119–1137.

[15] M. Durbeej, Laminins, Cell Tissue Res. 339 (1) (2010) 259–268.

[16] N.J. Gardiner, Integrins and the extracellular matrix: key mediators of development and regeneration of the sensory nervous system, Dev. Neurobiol. 71 (11) (2011) 1054–1072.

[17] M. Manthorpe, E. Engvall, E. Ruoslahti, F.M. Longo, G.E. Davis, S. Varon, Laminin promotes neuritic regeneration from cultured peripheral and central neurons, J. Cell Biol. 97 (6) (1983) 1882–1890.

[18] H. Colognato, P.D. Yurchenco, Form and function: the laminin family of heterotrimers, Dev. Dyn. 218 (2) (2000) 213–234.

[19] R.J. Riopelle, K.E. Dow, Functional interactions of neuronal heparan sulphate proteoglycans with laminin, Brain Res. 525 (1) (1990) 92–100.

[20] R. Sasisekharan, Z. Shriver, G. Venkataraman, U. Narayanasami, Roles of heparan-sulphate glycosaminoglycans in cancer, Nat. Rev. Cancer 2 (7) (2002) 521–528.

[21] M.A. Decoster, G.H. Devries, Evidence that the axolemmal mitogen for cultured schwann-cells is a positively charged, heparan-sulfate proteoglycan-bound, heparin-displaceable molecule, J. Neurosci. Res. 22 (3) (1989) 283–288.

[22] K. Forsten-Williams, C.L. Chu, M. Fannon, J.A. Buczek-Thomas, M.A. Nugent, Control of growth factor networks by heparan sulfate proteoglycans, Ann. Biomed. Eng. 36 (12) (2008) 2134–2148.

[23] D.A. Pye, R.R. Vives, P. Hyde, J.T. Gallagher, Regulation of FGF-1 mitogenic activity by heparan sulfate oligosaccharides is dependent on specific structural features: differential requirements for the modulation of FGF-1 and FGF-2, Glycobiology 10 (11) (2000) 1183–1192.

[24] H. Cui, M.J. Webber, S.I. Stupp, Self-assembly of peptide amphiphiles: from molecules to nanostructures to biomaterials, Biopolymers 94 (1) (2010) 1–18.

[25] K. Tashiro, G.C. Sephel, B. Weeks, M. Sasaki, G.R. Martin, H.K. Kleinman, Y. Yamada, A synthetic peptide containing the IKVAV sequence from the A chain of laminin mediates cell attachment, migration, and neurite outgrowth, J. Biol. Chem. 264 (27) (1989) 16174–16182.

[26] G.A. Silva, C. Czeisler, K.L. Niece, E. Beniash, D.A. Harrington, J.A. Kessler, S.I. Stupp, Selective differentiation of neural progenitor cells by high-epitope density nanofibers, Science 303 (5662) (2004) 1352–1355.

[27] V.M. Tysseling, V. Sahni, E.T. Pashuck, D. Birch, A. Hebert, C. Czeisler, S.I. Stupp, J.A. Kessler, Self-assembling peptide amphiphile promotes plasticity of serotonergic fibers following spinal cord injury, J. Neurosci. Res. 88 (14) (2010) 3161–3170.

[28] V.M. Tysseling-Mattiace, V. Sahni, K.L. Niece, D. Birch, C. Czeisler, M.G. Fehlings, S.I. Stupp, J.A. Kessler, Self-assembling nanofibers inhibit glial scar formation and promote axon elongation after spinal cord injury, J. Neurosci. 28 (14) (2008) 3814–3823.

[29] B. Mammadov, R. Mammadov, M.O. Guler, A.B. Tekinay, Cooperative effect of heparan sulfate and laminin mimetic peptide nanofibers on the promotion of neurite outgrowth, Acta Biomater. 8 (6) (2012) 2077–2086.

[30] G. Paxinos, K.W. Ashwell, I. Tork, Atlas of the Developing Rat Nervous System, Academic Press, 2013.

[31] M. Cansev, I.H. Ulus, L. Wang, T.J. Maher, R.J. Wurtman, Restorative effects of uridine plus docosahexaenoic acid in a rat model of Parkinson's disease, Neurosci. Res. 62 (3) (2008) 206–209.

[32] D. Kirik, C. Rosenblad, A. Bjorklund, Characterization of behavioral and neurodegenerative changes following partial lesions of the nigrostriatal dopamine system induced by intrastriatal 6-hydroxydopamine in the rat, Exp. Neurol. 152 (2) (1998) 259–277.

[33] D. Kirik, C. Rosenblad, A. Bjorklund, Preservation of a functional nigrostriatal dopamine pathway by GDNF in the intrastriatal 6-OHDA lesion model depends on the site of administration of the trophic factor, Eur. J. Neurosci. 12 (11) (2000) 3871–3882.

[34] T. Schallert, J.L. Tillerson, Intervention strategies for degeneration of dopamine neurons in Parkinsonism, Central nervous system diseases, Springer (2000) 131–151.

[35] M. Lundblad, M. Andersson, C. Winkler, D. Kirik, N. Wierup, M.A. Cenci, Pharmacological validation of behavioural measures of akinesia and dyskinesia in a rat model of Parkinson's disease, Eur. J. Neurosci. 15 (1) (2002) 120–132.

[36] M. Olsson, G. Nikkhah, C. Bentlage, A. Bjorklund, Forelimb Akinesia in the Rat Parkinson Model – Differential-Effects of Dopamine Agonists and Nigral Transplants as Assessed by a New Stepping Test, J. Neurosci. 15 (5) (1995) 3863–3875.

[37] O.A. Levy, C. Malagelada, L.A. Greene, Cell death pathways in Parkinson's disease: proximal triggers, distal effectors, and final steps, Apoptosis 14 (4) (2009) 478–500.

[38] P.D. Yurchenco, Y.S. Cheng, J.C. Schittny, Heparin modulation of laminin polymerization, J. Biol. Chem. 265 (7) (1990) 3981–3991.

[39] P.C. Georges, W.J. Miller, D.F. Meaney, E.S. Sawyer, P.A. Janmey, Matrices with compliance comparable to that of brain tissue select neuronal over glial growth in mixed cortical cultures, Biophys. J. 90 (8) (2006) 3012–3018.

[40] U. Ungerstedt, 6-Hydroxy-dopamine induced degeneration of central monoamine neurons, Eur. J. Pharmacol. 5 (1) (1968) 107–110.

[41] S. Moore, S. Thanos, The concept of microglia in relation to central nervous system disease and regeneration, Prog. Neurobiol. 48 (4–5) (1996) 441–460.

[42] W.E. Thomas, Brain macrophages – evaluation of microglia and their functions, Brain Res. Rev. 17 (1) (1992) 61–74.

[43] M. Hamanoue, N. Takemoto, K. Matsumoto, T. Nakamura, K. Nakajima, S. Kohsaka, Neurotrophic effect of hepatocyte growth factor on central nervous system neurons in vitro, J. Neurosci. Res. 43 (5) (1996) 554–564.

[44] T. Miwa, S. Furukawa, K. Nakajima, Y. Furukawa, S. Kohsaka, Lipopolysaccharide enhances synthesis of brain-derived neurotrophic factor in cultured rat microglia, J. Neurosci. Res. 50 (6) (1997) 1023–1029.

[45] J. Zhang, N. Niu, M. Wang, M.A. McNutt, D. Zhang, B. Zhang, S. Lu, Y. Liu, Z. Liu, Neuron-derived IgG protects dopaminergic neurons from insult by 6-OHDA and activates microglia through the FcgammaR I and TLR4 pathways, Int. J. Biochem. Cell Biol. 45 (8) (2013) 1911–1920.